Acta Ciencia Indica, Vol. XLI P, No. 1, 21 (2015)

NANOCRYSTALLINE Pt-DOPED TiO_2 THIN FILMS PREPARED BY SPRAY PYROLYSIS FOR HYDROGEN GAS DETECTION

R . M. THOMBRE

Mahatma Gandhi Arts, Science & Late N.P. Commerce College, Armori, Dist- Gadchiroli-441208 (M.H.), India

RECEIVED : 13 February, 2015

Nanostructured pure and Pt-doped TiO_2 thin films were prepared by chemical spray pyrolysis technique. Aqueous solution of $TiCl_36H_2O$ (0.01 M) was chosen as the starting solution for the preparation of pure TiO_2 thin film. Aqueous solutions of $PtCl_66H_2O$ (0.01 M) and $TiCl_36H_2O$ (0.01 M) were mixed in volume % of 1:99, 2.5:97.5 and 5:95 respectively to obtain Pt-doped TiO_2 thin films. The solutions were sprayed onto quartz substrate heated at 350°C temperature to obtain the films. These thin films were fired for one hour at 550°C. the sensing performance of these films was tested for various gases such as LPG, H_2, CO_2, ethanol, NH_3 and Cl_2 (1000 ppm). The pt-doped TiO_2 (1:99) was observed to be most sensitive (572) to H_2 at 400°C with high selectivity against other gases. Its response time was short (10 s) and recovery was also fast (14 s). to understand the reasons behind the gas-sensing performance of the films, their structural and micro structural properties were studied using X-ray diffraction and electron microscopy (FE-SEM and TEM), respectively. Thicknesses of all these samples were determined using Surface Profiler. The results are interpreted.

KEYWORDS : Spray pyrolysis techniques; TiO_2 thin films; hydrogen gas response.

INTRODUCTION

As hydrogen gas is tasteless, colourless and odourless, it cannot be detected by human beings. The low ignition energy and wide flammable range makes it easily inflammable and explosive. Therefore, rapid and accurate detection is necessary during the production, storage and use of hydrogen. It is also essential for monitoring/controlling the hydrogen concentration of nuclear reactors, coal mines and semiconductor manufacturing, etc. (Aroutiounian 2005; Buttner *et al* 2011; Hubert and Banach 2011). Various types of hydrogen sensors with different operating principles have been explored including the resistive type (Termick and Cavicchi 1991), thermoelectric (Matsumiya *et al* 2004), optical fibre (Okazaki *et al* 2003), surface acoustics wave (Jakubik *et al* 2003), carbon nanotuve (Wong *et al* 2003) and cantilever-based sensors (Baselt *et al* 2003).

A few semiconducting metal oxides ZnO, SnO_2, Cr_2O_3 have been studied extensively for detection of toxic, hazardous and combustible gases (Wagh *et al* 2006; Bari *et al* 2009; Patil *et al* 208, 2010, 2011). Recently, many efforts have been made to improve the gas sensor

performances. Titanium dioxide is a very useful material and has been extensively investigated for its gas sensitive behaviour, excellent dielectric property as well as catalysis applications (Chen *et al* 2004; Ruiz *et al* 2004; Suryawanshi *et al* 2008).

In reactions involving titania, oxygen vacancies are one of the major advantages of such material. However, for better sensing performances, titania is doped with a variety of additives, such as platinum. These additives enhance the material sensitivity and selectivity and reduce the response time and operating temperature of the sensing layer. The application of nanomaterials to the design of hydrogen gas sensor is nowadays one of the most active research fields. This is due to their high activity, high surface-to bulk ratio, good adsorption characteristics and high selectivity. The gas sensing mechanism involves chemisorptions of oxygen on the oxide surface, followed by charge transfer during the reaction between chemisorbed oxygen reducing and target gas molecules. However, the physical and sensing properties of semiconductor gas sensors are directly related to their preparation, *e.g*. particle size, sensing film morphology, crack surface (Ge *et al* 2007), and film thickness (Dayan and Phanichphant 1997; Sakai *et al* 2001; Zheng *et al* 2002; Liewhiran *et al* 2007) as well as sensing film characteristics.

In this article, we present the preparation and characterization of nanostructure pure and characterization of nanostructure pure and Pt-doped TiO_2 thin films and their gas –sensing properties. Nanostructure pure and Pt-doped TiO_2 thin films are prepared by spray pyrolysis deposition technique (SPD).

EXPERIMENTAL

2.1 Experimental set-up to prepare nanostructured thin films

Figure 1 shows a chemical spray pyrolysis technique for preparation of pure and Pt-doped TiO_2 nanocrystalline thin films. Set-up consists of spraying chamber, spray gun, air compressor, temp controller, and heater. Transparent conducting. Nonstoichiometric, nanocrystalline pure and Pt-doped TiO_2 thin films were prepared. The spray produced by nozzle was sprayed onto the glass substrates heated at 350+ 10°C. various parameters such as nozzle-to substrate distance, deposition time and flow tate of solution, deposition temperature and concentration were optimized to films in good quality.

2.2 Preparation of TiO_2 thin films

The spray pyrolysis technique was employed to prepare TiO_2 thin films. AR grade solution of $TiCl_3$ (0.01 M) was used as precursor. The solution was sprayed onto glass substrate heated at 350°C to obtain termed as SI.

2.3 Preparation of Pt-doped TiO_2 thin films

To prepare, platinum doped TiO_2 thin films, the solutions of AR grade $PtCl_6.6H_2O$ (0.01 M) and titanium chloride ($TiCl_3$) (0.01 M) were mixed in the volume % (1:99, 2.5, 97.5 and 5:95). The solutions were sprayed on to glass substrate heated at 350°C. These thin films were fired for one hour at 550°C. Table 1 shows the preparative conditions of nanocrystalline TiO_2 thin films using spray pyrolysis.

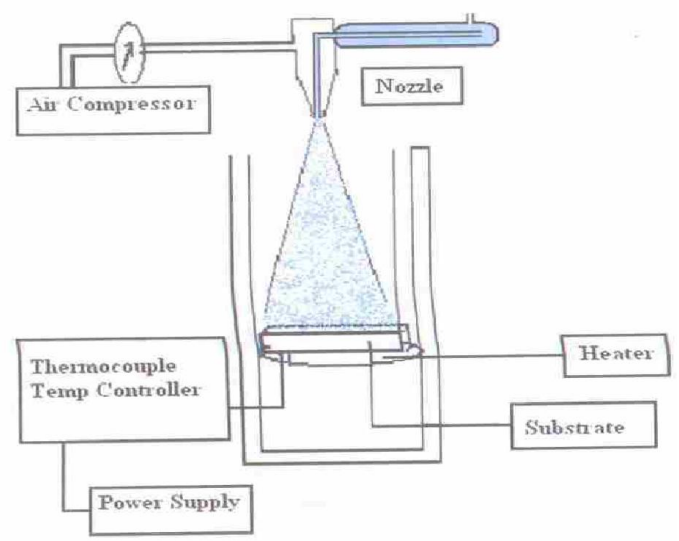

Fig. 1. Spray pyrolysis system set-up.

2.4 Thickness and roughness determination of thin films

The thickness and roughness of thin films were measured by using surface profiler (AMBIOS Tech. (USA) XP-I) having a vertical resolution of 1.5 A, lateral resolution of 100 nm and lateral length of 200 nm. The results are presented in table 2.

MATERIAL CHARACTERIZATIONS

As prepared nanostructured thin films were characterized by X-ray diffractometer using CuKa (y = 1.5418 A) radiation. The quantitative elemental analyses of the films were estimated by JEOL-energy dispersive spectrometer (model JED-2300). TEM images were recorded from transmission electron microscope (CM 200 Philips (200kV HT)). Thickness and roughness of thin films were measured by using surface profiler (AMBIOS Tech. (USA) XP-I). Electrical and gas sensing properties were measured using a static gas sensing system. The sensor performance on exposure of LPG, carbon dioxide, hydrogen, ammonia, ethanol and chlorine was examined.

3.1 Crystal structure using X-ray diffraction

Figure 2 represents the X-ray diffractograms of pure TiO_2 (S1) and Pt-doped TiO_2 (D1) thin films. The diffraction peaks from various planes and d-values are matching well with standard ASTM data, card no. 21-1272 of TiO_2. There are no prominent peaks of PtO associated in XRD pattern. It may be due to the smaller volume % of platinum doped in TiO_2. It reveals from XRD that the films are nanocrystalline in nature with anatase phase. All the peaks are corresponding to tetragonal TiO_2 with strongest (101) peak. The average crystallite size was calculated from (101) and (200) peaks, using Scherer formula and was found to be 12 nm for sample S1 and 18 nm for sample D1.

3.2 Elemental composition of pure and Pt-doped TiO_2 thin films

The quantitative elemental composition of pure TiO_2 and Pt-doped TiO_2 thin films were analyzed using an energy dispersive spectrometer and atomic % of O, Ti Pt is represented in

table 3. The samples are not perfectly stoichiometric, leading to semiconducting in nature (table 3).

Table 1. Preparation condition of TiO_2 and Pt-doped TiO_2 thin films.

Sample name	$PtCl_6$ (0.01 M) solution (ml)	$TiCl_3$ (0.01 M) solution (ml.)	Substrate temp. (OC)	Firing temp. (OC)
S1	00.00	100.00	350	550
D1	01.00	99.00	350	550
D2	02.50	97.50	350	550
D3	05.00	95.00	350	550

Table 2. Thickness and roughness of pure and Pt-doped TiO_2 thin films.

Sample Number	Film thickness (nm)	Film roughness (nm)
S1	223.80	33.30
D1	21.10	05.50
D2	43.80	13.12
D3	57.20	15.50

Table 3. Elemental analysis of pure and Pt-doped TiO_2 thin films.

Element	Pure TiO_2 (S1)	Pt-doped TiO_2 (D1)	Pt-doped TiO_2 (D2)
O	71.73	86.70	87.44
Ti	28.27	12.29	10.90
Pt	00.00	01.01	01.66
Total	100.00	100.00	100.00

3.3 Surface morphology of pure TiO_2 thin film

Figure 3 depicts the FE-SEM of sample S1 fired at 550°C for 60 min. pure TiO_2 thin film is observed to be continuous, dense and without any cracks and it consists of uniformly distributed grains having average crystallite size of 13 nm. The histogram shows grain size distribution is sample S1.

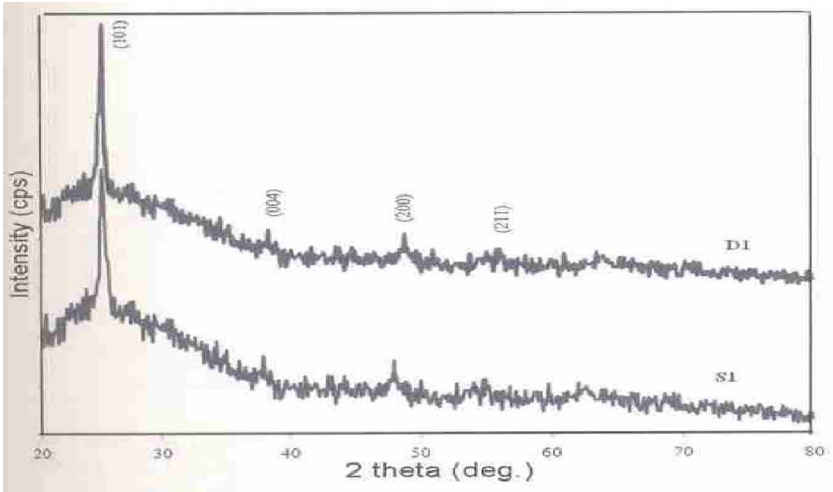

Fig. 2. XRD of pure (S1) and Pt-doped TiO_2 (D1) thin films.

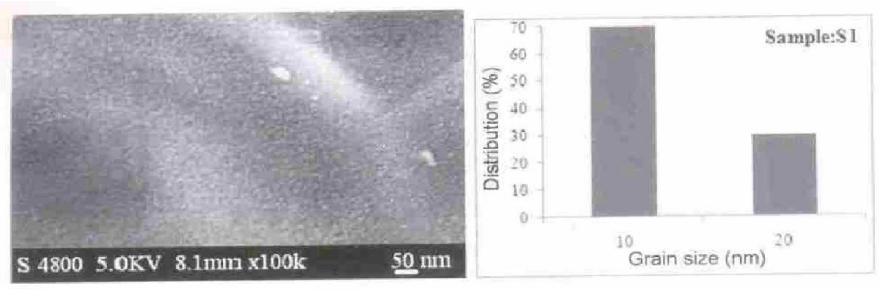

Fig. 3. FE-SEM image with histogram sample S1.

3.4 Surface morphology Pt-doped TiO_2 thin film

Figures 4(a) and (b) show surface morphology of D1 and D2 thin films, respectively. The histograms 4(C) and 4(d) show the grain size distribution in D1 and D2 samples. The grains of D1 are ellipsoidal in nature with an average grain size of 27 nm and D2 film consists of grains with an average grain size of 36 nm. it is clear from figures 4 (a) and (b) that some very small white particles are dispersed uniformly on the surface of both D1 and D2 films. The numbers of such particles are observed to be increasing with increase in Pt-doping concentration. These particles may be of platinum.

3.5 Transmission electron microscopy of pure and Pt-doped TiO_2 thin films

Figure 5(a) and (c) show the transmission electron microscopy (CM 200 Philips (200kV HT) of powders obtained by scratching the thin films of sample S1 and sample D1. The powder was dispersed in ethanol. Transmission microscopy uses copper grid to hold the powder. It is clear from TEM images that the grains are spherical in shape and nanocrystalline in nature with average crystallite size of 10.52 nm in case of S1 and 16.21 nm in case of D1. Additional structural characterization was carried out by electron diffraction shown in figures 5(b) and (d). Spherical rings in electron diffraction patterns suggest that the nanopowders have good crystallinity. The images show the clear fringes corresponding to the (101), (004), (200), (211), (204) and (116) lattice planes of TiO_2. It is clear from TEM images that there are nanocrystallites in the powders and turn in the films. The average crystalline size observed from XRD and grain size from TEM and FESEM are listed in table 4.

ELECTRICAL PROPERTIES OF THE SENSOR

4.1 I-V characteristics

Figure 6 shows I-V characteristics of nanostuctured pure and Pt-doped TiO_2 thin films. The graphs are observed to be symmetrical in nature indicating ohmic contact.

4.2 Electrical conductivity

Figure 7 shows the variation in electrical conductivity of thin film samples S1, D1, D2 and D3 with temperature. Electrical conductivity measurement for each film was made in the temperature range between 250 and 450°C in steps of 50°C. It is clear from the graphs that electrical conductivity goes on increasing with temperature for all samples.

4.3 Gas- sensing performance of the sensor

The gas-sensing performance of the nanostructured thin films was tested using static gas-sensing system explained elsewhere (Jain *et al* 2006).

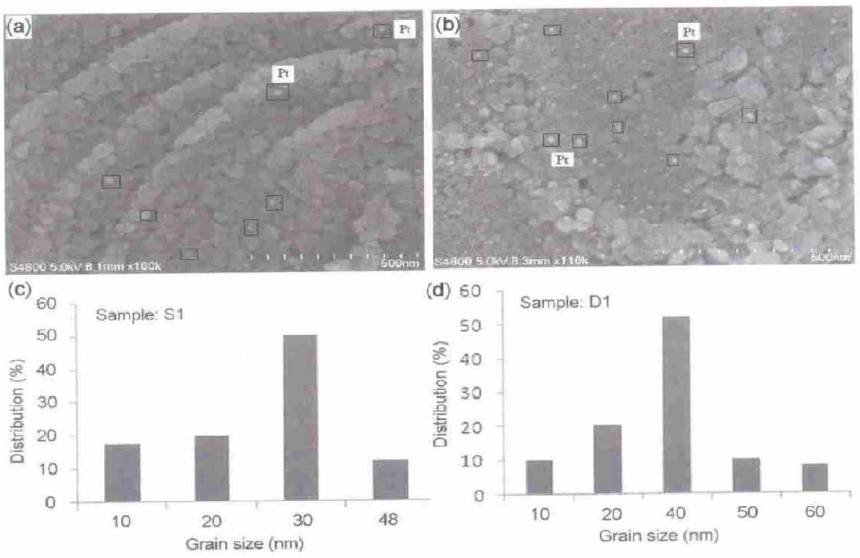

Fig. 4. FE-SEM images with histograms : sample D1 (a, c), sample D2 (b, d).

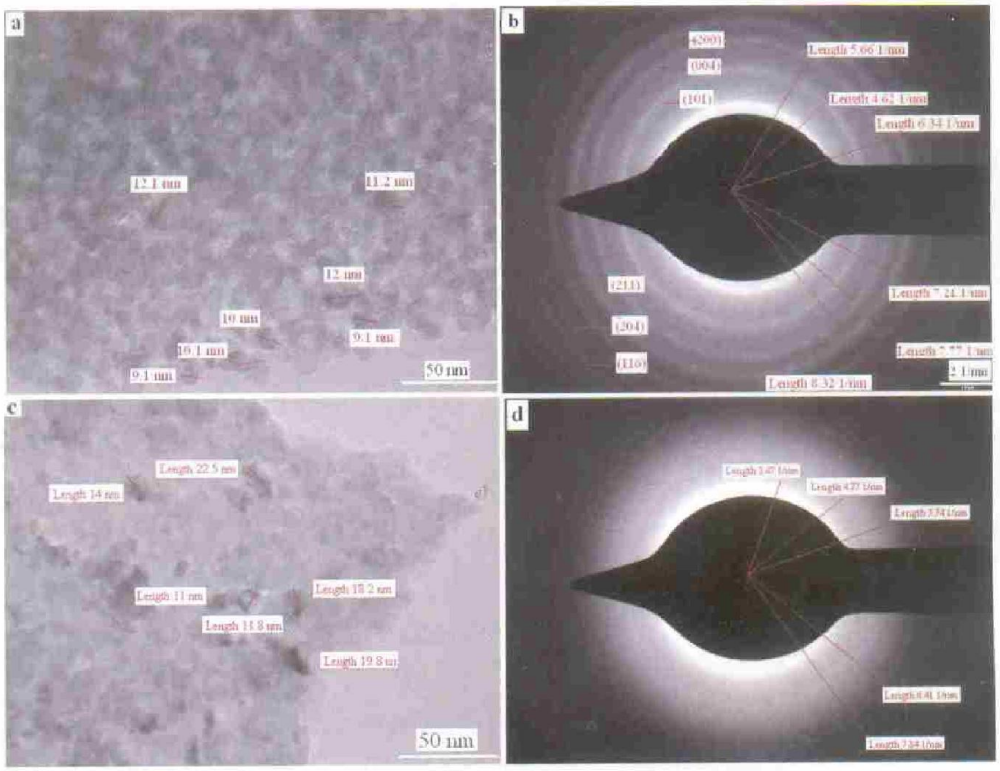

Fig. 5. TEM and electron diffraction images : sample S1 (a, b) and sample D1 (c, d).

4.4 Sensing performance of pure TiO_2 thin films

Figure 8 shows the variation of gas (1000 ppm) responses of pure TiO_2 thin film, the pure TiO_2 thin film showed highest response to LPG at 350°C (24) and H2 at 250°C (27). The same sensor responded to LPG and hydrogen, respectively at 350 and 250°C. Therefore, pure TiO_2 thin film showed temperature dependent sensing properties.

4.5 Sensing performance of Pt-doped TiO_2 thin film

Figure 9 shows variation in hydrogen response with operating temperature. It is clear form the figure that the gas response increases with operating temperature, reaches maximum (S = 578) at 400°C and then falls with further increase in operating temperature. Higher sensitivity of Pt-doped TiO_2 (D1) may be due to spill over action of platinum and nanocrystalline nature of film (16.21 nm). High surface to volume ratio (available due to nanocrystalline nature) allows gas to interact with latger surface are giving ultra large gas response (Young *et al* 1987).

Table 1 shows the thickness of sample D1 as 21.10 nm which is very small as compared to sample D2 and D3. It is clear from the reported data (Jin *et al* 1998: De *et al* 1999: Hammond and Liu 2001) that the gas sensitivity of nanocrystalline thin film increases with decreasing film thickness (Shukla and Seal 2003). The increase in the gas sensitivity with decrease in the film thickness can be explained on the basis of the model proposed by (Sakai *et al*).

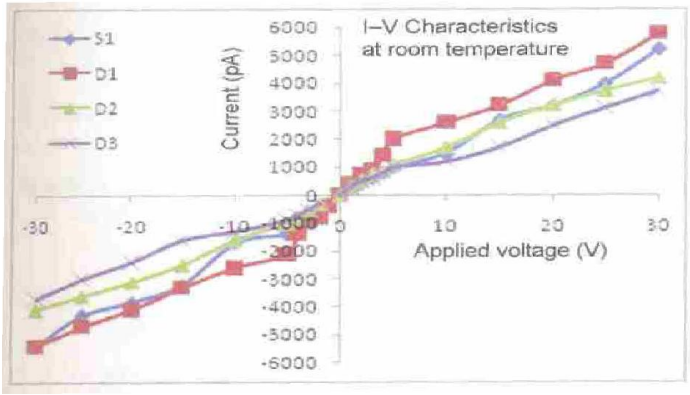

Fig. 6. I-V characteristics of Pt-doped TiO_2 thin films.

Table 4 Measurement of crystalline and grain size.

	Average crystalline size	Average grain size	
Sample name	XRD (nm)	TEM (nm)	FESEM (nm)
S1	12	10.52	13
D1	18	16.21	27

4.6 Selectivity

Sensing performances of the Pt-doped TiO_2 thin films (D1, D2, D3) were tested by exposing them with Wghnol, CO_2, Cl_2, LPG, H_2 and NH_3 gases.

Figure 10 shows selectivity of nonstructured Pt-doped TiO_2 thin films to H_2 against CO_2, LPG, NH_3, Cl_2 and ethnol gases at 400°C. It is clear from the figure that the nanostructured Pt-doped TiO_2 thin films were found to be highly selective to H_2 at 400°C against other gases.

4.7 Response and recovery of sensor

The time taken for the sensor to attain 90% of the maximum decrease in resistance on exposure to the target gas, is the response time. The time taken for the sensor to get back 90% of original resistance is the recovery time. The response and recovery of sensor (D1), on exposure of 1000 ppm of H_2 at 400°C, are represented in figure 11. The response time of the sensor was observed to be (10 s) and the recovery time was (14 s). sensor showed quick response and fast recovery.

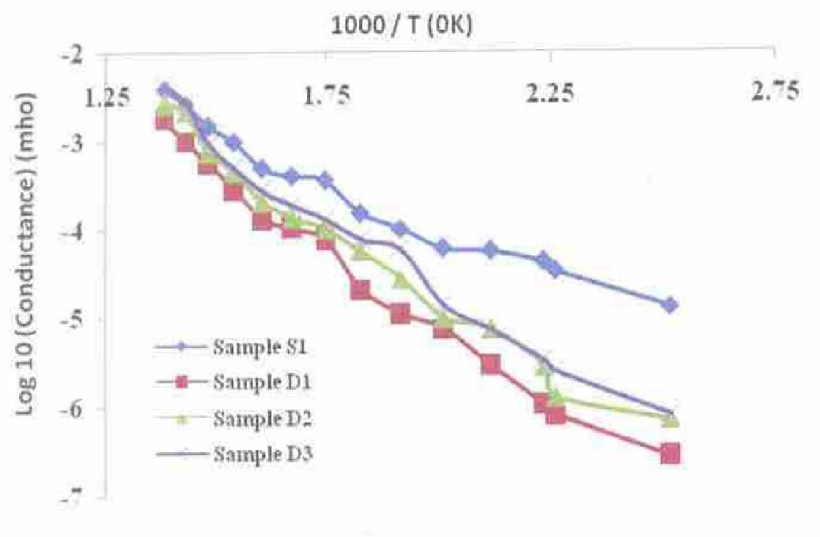

Fig. 7. Conductivity-temperature profile.

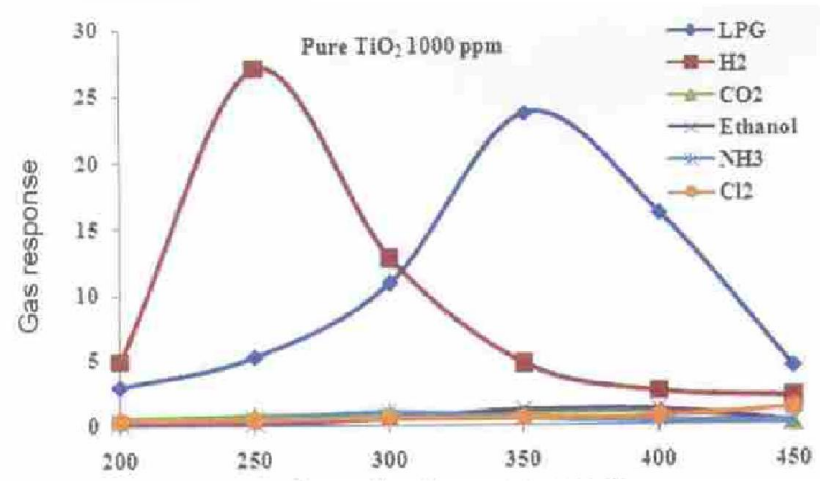

Fig. 8. Operating temperatue (°C)

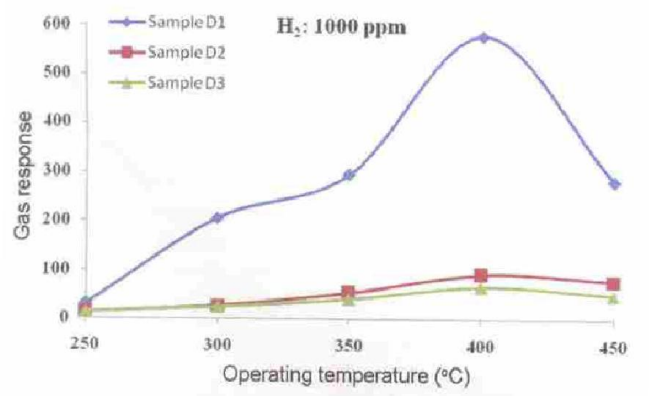

Fig. 9. H_2 gas response-operating temperature profile.

Discussion

The most important features of the present investigation are: high gas response, high selectivity to hydrogen against other gases, fast response and quick recovery. The enhanced response could be attributed to nanocrystalline nature of the films. It is known that, when nanocrystalline Pt-doped TiO_2 semiconductor thin film is exposed to air, conduction band of Pt-TiO_2 and change to O_{2ads} of O_{ads} species (Morrison *et al* 2001) as indicated in (1) (2):

$$O_2 \text{ (gas)} + e \text{ ---------- } O_2 \text{ (ads)}, \quad \ldots (1)$$

$$O_2 \text{ (ads)} + e \text{ --------- } 2O \text{ (ads)} \quad \ldots (2)$$

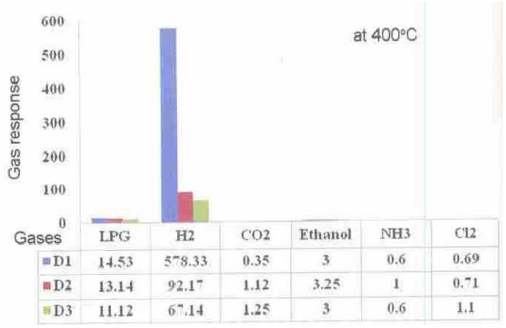

Gases	LPG	H2	CO2	Ethanol	NH3	Cl2
D1	14.53	578.33	0.35	3	0.6	0.69
D2	13.14	92.17	1.12	3.25	1	0.71
D3	11.12	67.14	1.25	3	0.6	1.1

Fig. 10

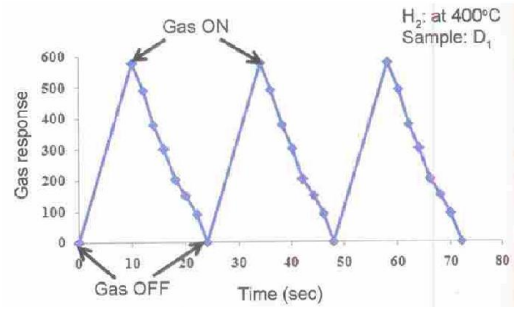

Fig. 11. Response and Recovery of sensor

The adsorption of O_2 and O ions on the nanocrystalline Pt-doped TiO_2 surface is vital to enhance the receptor function of the sensor and, hence, its gas response. The receptor function is an ability of metal oxide surface to receive the target gas, which is directly related to surface capability to adsorb O_2 and O ions. Larger the ability of the surface to receive and oxidize the target gas, larger could be the change in conductivity of the sensor and, hence, enhancement in gas response. Number of O_2 and O ions adsorbed on the surface also depends on oxygen-ion vacancies within the Pt- doped TiO_2 lattice. Oxygen-ion vacancies , within the Pt-doped TiO_2 lattice, can result in increased adsorption of the oxygen-ions (O_2 an O ions) on the sensor surface. Any mechanism that can in crease the lattice oxygen-ion vacancy concentration can lead to significant increase in both the receptor function and the gas response of the nanocrystalline Pt-doped TiO_2 sensors.

The interacation between adsorbed O_2 and O ions (on the Pt-TiO_2 surface) and hydrogen, target gas, can be explained in terms of reactions (3) and (4) as follows:

$$2H + O_2\,(ads) = 2H_2O + e \quad \ldots (3)$$

or

$$H_2 + O\,(ads) = H_2O + e \quad \ldots (4)$$

In addition, the usage of nanostructures increases the surface to volume ratio which generally enhances the sensor response. The increase in the surface area of nanostructured materials can also lead to increase in catalytic activity or surface adsorption.

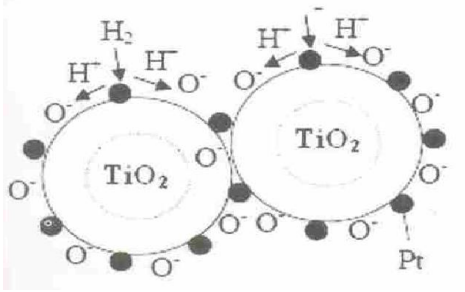

Fig. 12. Gas sensing mechanisms based on'spill over' effect of Pt-doped TiO_2 nanoparticles.

It is widely believed that Pt-catalyst enhances reducing gas sensing of metal oxide via spillover mechanism (Morrison 1982). This interaction is a chemical reaction by which additives assist the redox process of metal oxides. The term 'spill over' refers to the process, illustrated in figure 12. In this process, the metal catalyst dissociates from the molecule and then the atom can 'spill over' onto the surface of the semiconductor support. At appropriate temperatures, reactants are first adsorbed on to the surface of additive particles and then migrate to the oxide surface to react there with surface oxygen species, affecting the surface conductivity. For the above processes to dominate the metal oxide resistance, the spilled-over species must be able to migrate to the interparticle contact. Thus, for a catalyst to be effective, there must be a good dispersion of the catalyst so that catalyst particles are available near all contacts. Only then can the catalyst affect the important interparticle contact resistance.

Conclusions

Chemical spray pyrolysis technique is simple, convenient, and 'green': it may be used to large scale industrial application for preparation of nanostructured metal oxides. Because the nanostructured thin films and nanoparticles have large surface areas, stable structure, and a particular inner environment, such materials may find great applications in gas sensing,

heterogeneous catalysis, optical devices, and micro reactors. Very high resistance before exposure of target gas and very low resistance in presence of target gas are the most important characteristics of nanocrystalline Pt-doped TiO_2 thin films. Pure TiO_2 thin film shows maximum gas response to H_2 (27). Addition of Pt was observed to enhance sensitivity of the Pt-doped TiO_2 thin film to hydrogen gas were observed to be extremely high in comparison to NH_3, CO_2, Cl_2, LPG and C_2H_5OH. The enhanced gas response could be attributed to nanocrystalline nature of the films. Hydrogen gas response of the present nanocrystalline Pt-doped TiO_2 thin film sensor may be due to the simultaneous activation of its receptor (due to the adsorption of O_2 and O ions on the surface) and transducer (due to the 'grain control' resistance mechanism) functions.

References

1. Chrisai, Stoulakis S., Suchea, M., Koudoumas, E., Katharakis, M. and Katsarakis, N., *Appl. S.,* **5351** (2006).
2. Ge, D., Xie, C. and Cai, S., *Mater. Sci. Eng.,* **B13,** 753 (2007).
3. Hubert and Banach, L. G., *Sensors & Actuators,* **B157,** 329 (2011)
4. Drnovsek, J., Kuscer, S., Macek, D. and Kosed, S., *J. Eur.,* **26,** 2985 (2006).
5. Patil, D. R. and Patil, L. A., *Sensors & Transducers,* **81,** 1354 (2007).
6. Patil, L. A., Shinde, M. D., Bari, A. R. and Deo, V. V., *Sensors and Actuators,* **B143,** 316 (2009).
7. Patil, L. A., *Sensors and Transducer,* **104,** 68 (2009).
8. Patil, L. A., Shinde, M. D., Bari, A. R. and Deo, V., *Sensors & Actuators,* **B143,** 270 (2009).
9. Patil, L. A., Shinde, M. D., Bari, A. R. and Deo, V., *Curr. Appl. Phys.,* **10,** 1249 (2010).
10. Patil, L. A., Shinde, M. D., Bari, A. R. and Deo, V., *Mater. Sci. Eng.,* **B176,** 579 (2011).
11. Patil, S. A., Patil, L. A., Patil, D. R., Jain, G. H. and Wagh, M. S., *Sensors & Actuators,* **B123,** 233 (2007).
12. Suryawanshi, D. N., Patil, D. R. and Patil, L. A., *Sensors & Actuators,* **B134,** 579 (2008).
13. Wang, M. S., Jain, G. H., Patil, D. R., Patil, S. A. and Patil, L. A., *Sensors & Actuators,* **B115,** 128 (2006).

❑